Experimental Study of Secondary Imperfections at the Welds of a Model Spherical Containment

F.W. Bornscheuer
Universität Stuttgart, Institut für Baustatik,
Pfaffenwaldring 7, D-7000 Stuttgart 80, Germany

Abstract

The paper describes the experimental investigation of a model spherical containment with a diameter of 2.6 m. Two experiments were performed. The shell with one protruding nozzle had been welded using a high strength steel. The model has a wall thickness of 30 mm which is also the thickness of the real containment with a diameter of 56 m. The structure has an equatorial butt weld with a heart-shaped necking. This geometrical imperfection at the butt weld and the small weld radius at the fillet weld between the nozzle and the spherical containment leads to local strain concentrations if the structure is pressurized. The welds had been weakened by further imperfections caused by undergrinding or undercutting. These additional imperfections produce extra strain concentrations which were measured and determined by a nonlinear finite element analysis. The strain functions allow certain conclusions for the limit load of the structure.

1. Introduction and Scope of the Study

At the welds of PWR-containments geometrical deviations of the ideal spherical shape may occur. These are essentially mismatches and heart-shaped necking of the welds. These geometrical imperfections cause strain concentrations if internal pressure is applied. A similar strain state may occur at the intersection zone of a cylindrical nozzle and the spherical containment. Experimental and analytical investigations on the influence of these geometrical imperfections are described in [1] and [2].

During occasional check-ups or routine supervision small, not yet discovered material defects, for example cracks, may be detected. These faults are usually removed by grinding. If this repairing process leads to a smooth, not too deep and not too extended groove the rewelding can be omitted. Often the undergrinding is located in the weld where the above mentioned primary strain concentrations are present. In these areas the secondary strain concentrations caused by the undergrinding have to be superimposed. They may be defined as secondary geometrical imperfections. The excessive strains are related to extreme stresses which may already reach the yield limit when the load is still in the lower range. The stress concentrations do not allow to judge the load carrying capacity of the structure.

It is the purpose of this paper to determine the ultimate load of the model structure under internal pressure when secondary geometrical imperfections are present. The investigation is based on measured strain concentrations as well as on corresponding elasto-plastic finite element analyses. The model sphere shown in figure 1 a) has a diameter of 2.6 m and a wall thickness of 30 mm. The shell has one protruding cylindrical nozzle with an outer diameter of 750 mm. The material of the model sphere is a high strength vanadium alloyed steel with a minimum yield limit of 500 N/mm^2 within the wall of 30 mm thickness.

The test investigating the influence of the secondary imperfections was carried out recently at the Materialprüfungsanstalt of the University of Stuttgart.

2. Undergrinding of a Butt Weld

In addition to a heart-shaped necking of the equatorial butt weld No. III the thickness was locally reduced by grinding as shown in figure 1 b). The maximum reduction was 12 - 14 mm that is approximately half of the weld thickness of 30 mm. The length of the undergrinding was about 400 mm that is 1/20 of the circumference of the sphere. This reduction of the wall thickness is far more than usually tolerated. In the experiment the internal pressure was increased stepwise. Before applying the next load step the structure was unloaded. At many points of the weakened weld zone the strains were measured by strain gages.

Figure 2 shows a pressure - strain diagram of a highly stressed point of the undergrinding. The load increase was stopped when the maximum total strain reached the value of 2 %. The limit pressure obtained in the test was 135 bar.

In figure 3 the experimental pressure - strain function is being supplemented by a corresponding analytical result. The corresponding finite element mesh using an axisymmetric 8-node isoparametric element is shown in figure 5. The element was implemented in the program NISA [3]. The elasto-plastic finite element analysis was performed for an undergrinding of the entire circumference with a depth of 13 mm. This extreme case allows an axisymmetric computational model. Since the thin zone could be supported by the surrounding not weakened area a higher pressure could be obtained in the experiment for the same strain. The axisymmetric analysis does not include this supporting effect.

3. Undercut at the Fillet Weld of the Nozzle

At the transition zone of the fillet weld and the cylindrical nozzle a groove-shaped undergrinding was applied artificially as shown in figure 4 a) and 4 b). The nozzle has a wall thickness of 35 mm, the undercut has a radius of 5 mm and a depth of 3 mm. The length of this imperfection measured approximately 500 mm that is 1/5 of the entire circumferential weld.

The above mentioned imperfection of the equatorial weld No. III was rewelded so that an undergrinding of only 6 mm remained (figure 4 c)). This wall reduction is more realistic than the exaggerated 12 to 14 mm of section 2.

Again the internal pressure was increased stepwise and the strains were measured at both secondary imperfections, at the equatorial and the nozzle weld. Selected pressure - strain functions are plotted in the figures 6 and 7. The maximum internal pressure of 180 bar leads to a total strain of 2, 2 % for the fillet weld (figure 6) as well as the equatorial weld (figure 7).

Elasto-plastic finite element analyses were performed in addition to the experimental investigation, again using an axisymmetric computational model. The analytical and the experimental results do not agree very well as indicated by the load - strain diagram in figure 8 a). In particular distinct differences can be recognized in the elastic range for a low pressure level. The disagreement may be attributed to the relatively coarse finite element mesh of the fillet zone. Therefore, the experimental and analytical load - strain functions have been calibrated in figure 8 b) so that they agree in the elastic range. Now the analytical function leads to lower pressure values because the supporting effect is missing in the axisymmetrical analysis.

4. Discussion of the Results

In addition to deviations of the ideal spherical geometry leading to primary strain concentration further geometrical imperfections have been considered in both experiments of the model sphere. These secondary or accidental imperfections cause additional strain concentrations.

In both tests the internal pressure was increased so that the maximum total strains of the groove root did not exceed approximately 2 %. The pressure strain functions allow the conclusion that the value of 2 % is not a limit strain. The pressure even could be increased more considerably. Obviously this positive response is based on the fact that the extremely high strained parts of the structure have a local character. During the tests it could be observed that in the neighbouring areas the strains decay rapidly. Numerical analyses in which certain parameters are varied may even allow a more detailed judgement of the influence of the secondary imperfections. For example figure 8 clearly shows the differences between the load - strain functions of the structure with and without undergrinding at the nozzle. Both functions converge to two different limit pressures. The reduction of the ultimate load of the structure with the undergrinding is approximately 10 %.

Furthermore, the different representations of the Bauschinger effect should be noted. Based on the same total strain the Bauschinger effect is considerably higher at the imperfect fillet weld of the nozzle (figure 6) than at the imperfect butt weld (figure 7). This is of minor importance for non-cyclic loading. If the maximum pressures are in the lower range no difference can be recognized for cyclic loading. Between the static loading 1000 cyclical load variations up to 40 bar were applied. These cyclic loads had no influence on the strains of the concluding static loading.

References

[1] BORNSCHEUER, F. W.: "Experimental Study of a Spherical PWR-Containment with Geometrical Imperfections at the Welds". SMiRT 5, Berlin, Vol. J, paper J 6/7, 1979.

[2] SÄTTELE, J. M., RAMM, E., BORNSCHEUER, F. W.: "Elasto-Plastic Analysis of Nozzle Intersections in Reactor Containments". SMiRT 5, Berlin, Vol. J, paper J 6/9, 1979.

[3] HÄFNER, L., RAMM, E., SÄTTELE, J. M., STEGMÜLLER, H.: "Programmdokumentation - Programmsystem NISA 80". Bericht, Institut für Baustatik, Universität Stuttgart, 1980.

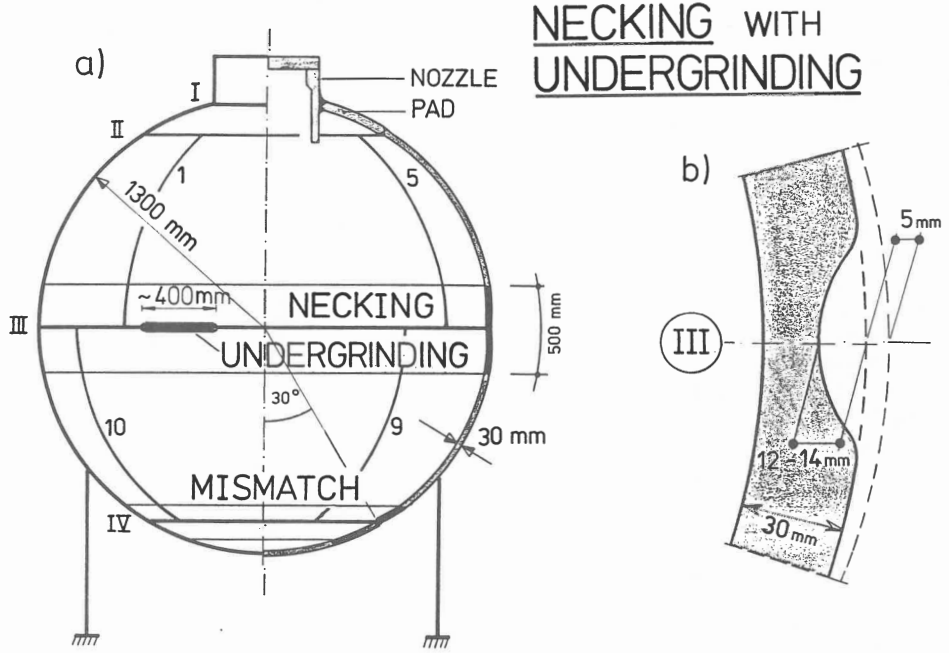

Figure 1: Spherical Model Shell with the weakened weld No. III

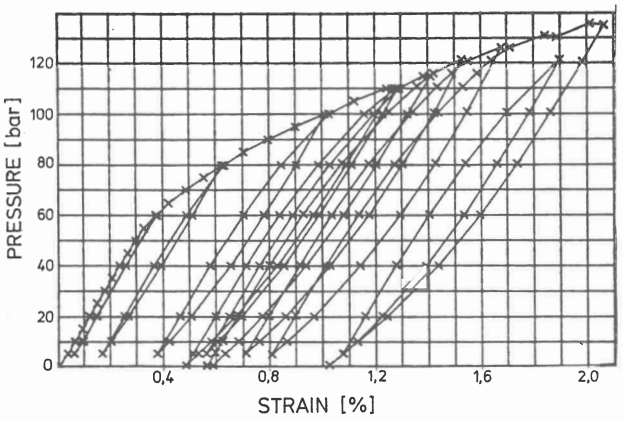

Figure 2: Load - strain diagram of the weakened weld No. III

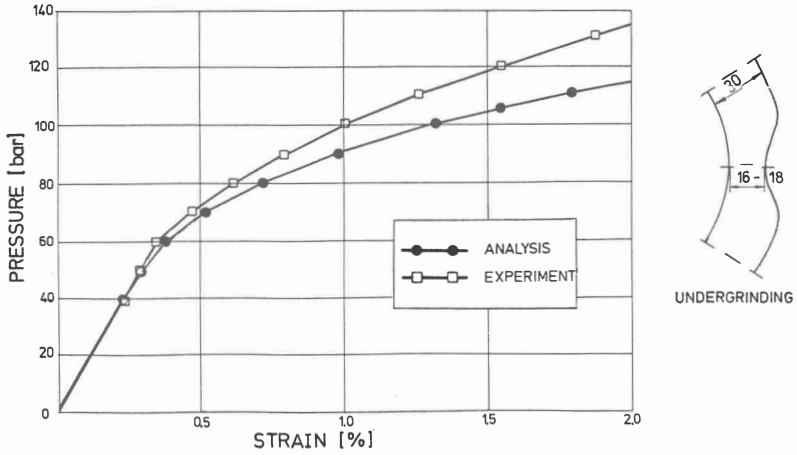

Figure 3: Load - strain diagram of the weakened weld No. III; comparison experiment / analysis

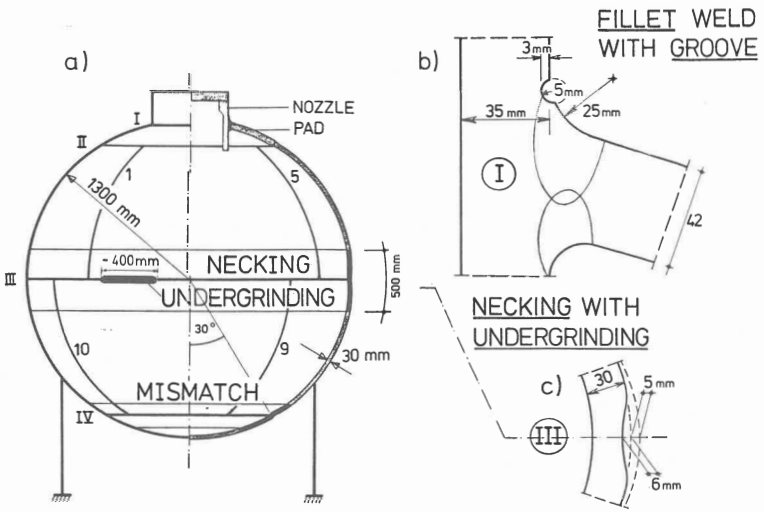

Figure 4: Spherical model shell with the weakened welds No. I and III

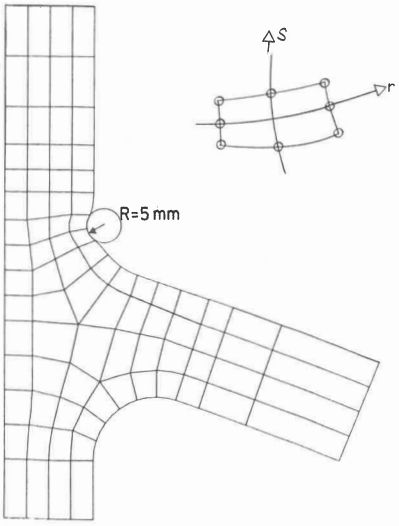

Figure 5: Thick shell idealization of the intersection zone

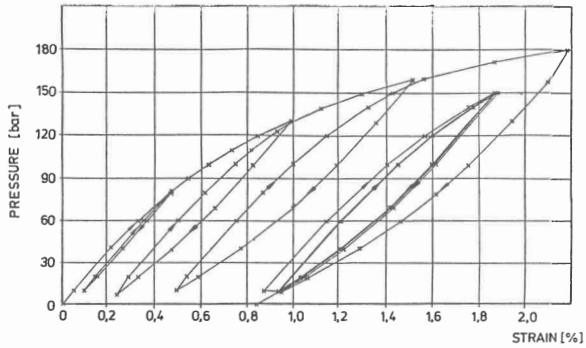

Figure 6: Load - strain diagram of the weakened weld No. I

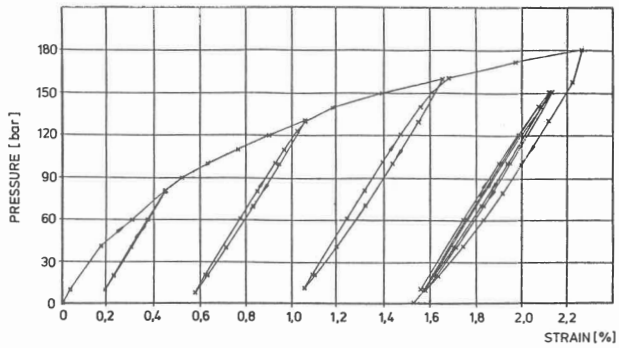

Figure 7: Load - strain diagram of the weakened weld No. III

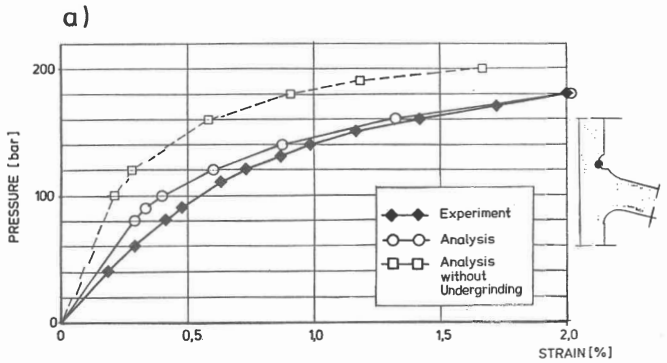

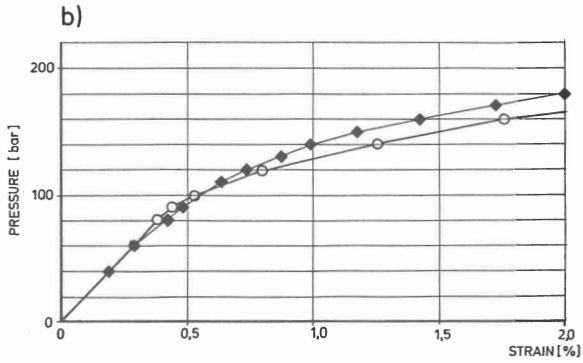

Figure 8: Load - strain diagrams of the weakened weld No. I; comparison experiment / analysis